A large enantiornithine bird from the Lower Cretaceous of China and its implication for lung ventilation

ZIHUI ZHANG[1*], DEFENG CHEN[2], HUITAO ZHANG[2] and LIANHAI HOU[1,3]

[1]*College of Life Sciences, Capital Normal University, Beijing 100048, China*
[2]*School of Mathematical Sciences, Capital Normal University, Beijing 100048, China*
[3]*Institute of Vertebrate Paleontology and Paleoanthropology, Chinese Academy of Sciences, Beijing 100044, China*

The Enantiornithes were the most taxonomically diverse bird group in the Mesozoic. Most of the known taxa are from Lower Cretaceous deposits of the Jehol Group in north-eastern China. A new specimen from the Jiufotang Formation in Jianchang, Liaoning Province, is described here; being a subadult individual at the time of death it had reached a relatively large size. The presence of uncinate processes, bicapitate and forked vertebral ribs, sternal ribs that were all of similar length, as well as the location of parapophyses and diapophyses on the thoracic vertebrae, may imply a rigid and volume-constant lung, and less efficient lung ventilation in enantiornithines. © 2014 The Linnean Society of London, *Biological Journal of the Linnean Society*, 2014, **113**, 820–827.

ADDITIONAL KEYWORDS: Jianchang – Jiufotang Formation – Liaoning province – respiratory apparatus – ribs – thoracic vertebrae.

INTRODUCTION

The Enantiornithes were the most dominant and diverse clade of Mesozoic birds and occurred nearly worldwide throughout the entire span of the Cretaceous (Chiappe, 2007; Chiappe & Dyke, 2007; Dyke & Nudds, 2009). These birds had undergone extensive differentiation and radiation in size, morphology, diet, and flight capability by the Early Cretaceous (Dyke & Nudds, 2009; Wang & Zhang, 2011). The vast majority of Enantiornithes were small birds, between the size of a sparrow and a starling (Zhang & Zhou, 2000; Wang & Zhang, 2011; Zhang *et al.*, 2013). However, some large-sized enantiornithines from the Lower Cretaceous Jehol Group, such as *Aberratiodontus wui*, *Pengornis houi*, *Xiangornis shenmi*, and *Zhouornis hani*, document the significant size disparity of enantiornithines during the Early Cretaceous (O'Connor, 2009). Our new specimen, reported here, was a subadult individual and obviously larger than other enantiornithines. With more than 30 years of work on nearly 60 taxa of Enantiornithes, many

species are suggested to be good fliers and are well understood regarding their general lifestyle, reproductive biology, and growth strategies (Chiappe & Walker, 2002; Cambra-Moo *et al.*, 2006; Zheng *et al.*, 2013). It is without doubt that the evolution of flight in birds required the development of efficient respiratory and gas-exchange systems (Maina, 2006). The respiratory system of birds is composed structurally of two different parts: the lung (the gas exchanger) and the mechanical ventilator (the air sacs) (Fedde, 1980; Maina, 2006). The generation of unidirectional air flow through the lung relies primarily on the caudal air sacs (abdominal and caudal thoracic) and pressure differences between cranially and caudally positioned air sacs (Powell, 2000; Maina, 2006; Claessens, 2009). The vertebral ribs, sternal ribs, the sternum, and the thoracic vertebrae contribute to the ventilatory mechanism. Upon inspiration, the thorax expands in all dimensions. The vertebral ribs swing forward and upward, thereby increasing the transverse diameter of the trunk. The consistent location of the parapophysis throughout the dorsal vertebral series, ventral and cranial to the diapophysis, ensures a relatively uniform lateral expansion. An increase in the angle between the vertebral and the sternal ribs

---

*Corresponding author. E-mail: zihuizhang@cnu.edu.cn

causes the sternal ribs to push the sternum ventrally. Owing to the greater length of the caudal sternal ribs, the caudal sternal margin is displaced further ventrally than the cranial sternal margin (Claessens, 2009). Few studies have focused on the evolution of avian respiration and thus the information available in the literature is limited. Previous research has suggested an unmodified septate lung and a flow-through respiratory system in basal birds, such as *Archaeopteryx* and enantiornithines. Mechanisms for powering lung ventilation rely principally on pelvic and tail movements (Ruben *et al.*, 1997; Ruben, Jones & Geist, 2003) or mechanical advantage conferred by uncinate processes (Tickle, Norell & Codd, 2012). The morphology of the sternal and vertebral ribs, as well as the thoracic vertebrae, revealed in enantiornithines, gives us the opportunity to reconstruct the lung and lung ventilation of these early birds. The anatomical nomenclature used in this short paper follows that of Baumel & Witmer (1993).

SYSTEMATIC PALAEONTOLOGY

AVES LINNAEUS, 1758

ENANTIORNITHES WALKER, 1981

Enantiornithes Indet.

Material: Capital Normal University (CNU), Beijing, China, collection number VB-1001, a near-complete articulated skeleton of a subadult individual (Fig. 1).

Locality and horizon: Jianchang County, Liaoning Province. Jiufotang Formation, Lower Cretaceous, approximately 120 Mya (He *et al.*, 2004).

Enantiornithine diagnosis: This new bird can be referred to Enantiornithes because of the presence of a Y-shaped furcula with a long hypocleideum, a broad dorsal fossa on the sternal half of the coracoid, a supracoracoid nerve foramen opening into a medial furrow, a radius with a longitudinal groove on the interosseous surface of its shaft, a minor metacarpal projecting distally more than the major metacarpal, and a slender metatarsal IV compared with metatarsals II and III (Chiappe & Walker, 2002).

Description: The skull of CNU VB-1001 is crushed, primarily exposed in lateral view, and probably overlapped by soft tissues (Fig. 1). Little more information can be gained from this specimen apart from the following salient points: the antorbital fossa is triangle-shaped and smaller than the orbit cavity; the rostrum is nearly half the length of the total skull; and the skull roof is domed. This new bird possesses at least eight cervical vertebrae, which are mainly


Figure 1. The new material of Enantiornithes from the Lower Cretaceous in China (CNUVB-1001). cg, capital groove; co, coracoid; dc, deltopectoral crest of humerus; fe, femur; fi, fibula; fu, furcula; h, humerus; mi, minor metacarpal; ma, major metacarpal; r, radius; rg, radial groove; sl, semilunate carpal; sr, sternal rib; st, sternum; ti, trabecula intermedia; tib, tibia; tl, trabecula lateralis; tmt, tarsometatarsus; u, ulna; ul, ulnare; up, uncinate process; vr, vertebral rib; vt, ventral tuberosity; I–IV, digits I–IV. Scale bar equals 1 cm.

preserved in ventral view; the corpus of these vertebrae are more expanded cranially than caudally and they are constricted in their mid-section. The centrum of the fifth cervical vertebra is the longest and clearly has a concave facies articularis cranialis and convex facies articularis caudalis on its ventral side. The third cervical vertebra is nearly quadrate in form, having an osseous bridge from the ansa costotransversaria to the zygapophysis caudalis. Judging from computed tomography (CT) images of this region, the zygapophysis caudalis and the zygapophysis cranialis of the fifth to eighth cervical vertebrae are nearly the same in length; the angle between the left and the right zygapophysis caudalis

is a little smaller than that of the zygapophysis cranialis. The thoracic vertebrae are disarticulated and poorly preserved, so the exact number is unclear, but the articular facets are flat; the sides of the centra are deeply excavated by large longitudinal fossae. At least four free caudal vertebrae are discernable proceeding before the pygostyle; the centra of these caudals are short and bear elongated processus transversus, which point posterolaterally. The pygostyle is partly preserved, lacking its caudal element.

The rostral edge of the sternum presents as a caudally obtuse angle of approximately 110°. The lateral borders of the sternum are straight, parallel, and continuous with a long trabecula lateralis that lacks an obvious expanded distal end and appears to extend past the caudal end of the main body of the sternum. The right trabecula intermedia is discernable in CT images; it is thinner and shorter than the trabecula lateralis and has a distal end that terminates in the same transverse plane as the median xiphoid process. The ventral surface of the sternum is flat with no Carina sterni, and the left lateral border is preserved in articulation with four sternal ribs (Fig. 1). The caudal-most sternal rib is floating, attaching to the former one (as in modern birds) and at least the first three left ribs are completely preserved, with their vertebral and sternal components in articulation. Observation on these ribs indicates that the vertebral ribs were bicapitate and strongly forked and that the sternal ribs are nearly the same length. Three uncinate processes are preserved and attached to the middle part of the vertebral rib (Fig. 1).

Both coracoids of CNU VB-1001 are exposed in ventral view. The shoulder half is slender and laterally compressed; there is no presence of the processus procoracoideus. The supracoracoidal nerve foramen, discernable only in CT images, is elongate and lies on the medial border of the shaft below the omal end (Fig. 2). The distal half of each coracoid expands greatly and has a triangular-shaped outline; the ventral surface is convex to some extent and the sternal border is relatively straight. Both scapulae are clearly visible in the CT images, although the right scapula is completely concealed by the matrix and some other structures. The right and the left scapulae are preserved in costal and lateral views, respectively, and, in both, the glenoid facet is large and slightly concave. The acromion is well-developed and hook-shaped with a pointed end (Fig. 2), similar to *Pengornis* (Zhou, Clarke & Zhang, 2008). The furcula is Y-shaped with a developed hypocleideum missing its distal end; the ramus is robust and has little caudal excavation visible, again in the CT images. The interclavicular angle of the furcula is approximately 70°.
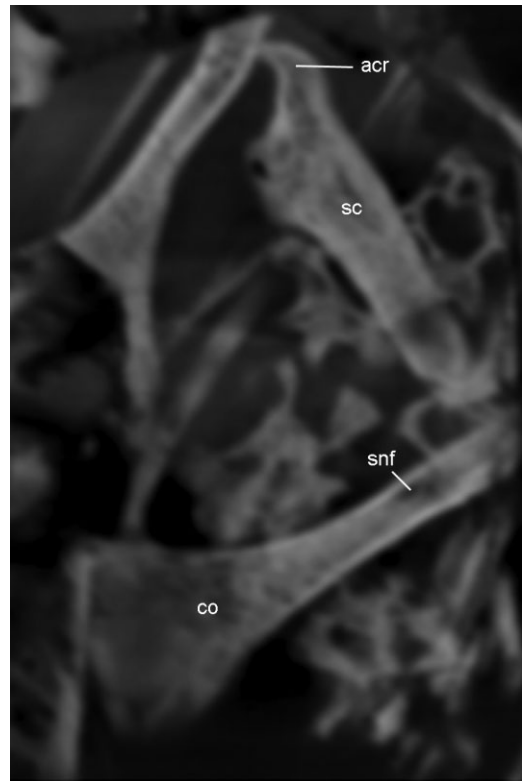
Figure 2. CT segmentation photography of the scapula and coracoids. acr, acrocoracoidal process; co, coracoid; sc, scapula; snf, supracoracoidal nerve foramen.

Both humeri of CNU VB-1001 are preserved in caudal view. The caput humeri is large, convex proximally and caudally, and the deltopectoral crest projects dorsally as a flat crest along about one-third of the length of the bone. The ventral tuberiosity is large and separated from the head by an obvious and deep capital groove (Fig. 1). The shaft of the humerus is relatively straight and its long axis is nearly perpendicular to the transverse axis of the distal end, which is less expanded compared with most enantiornithines. The olcranal fossa is relatively long and is located more ventrally rather than dorsally. The right ulna is well-preserved and curves, although slightly, towards the caudal end for most of its length and, as a result, a long and obvious interosseous space is present between the ulna and the straight radius. The ulna bears a short olecranon on its proximal end, but shows no evidence of papillae for the insertion of secondary remiges on the caudal margin. The right radius is preserved in caudal view and exhibits a distinct groove at the proximal half (Fig. 1), as in several enantiornithines such as *Eoenantiornis*, *Bohaiornis*, *Zhouornis*, *Parabohaiornis*, and *Longusunguis* (Chiappe & Walker, 2002; Zhou, Chiappe & Zhang, 2005; Hu *et al.*, 2012; Zhang

et al., 2013; Wang *et al.*, 2014). The diameter of the radius is nearly the same for its whole length, about three times less than that of the ulna. Preserved in the left forelimb, there is an incompletely fused semilunate carpal, which caps the proximal ends of three metacarpals. The shaft of the major metacarpal is straight, robust, and exhibits a longitudinal groove on its caudal surface. The minor metacarpal is relatively thin and bow-shaped, with its distal end surpassing that of the major metacarpal, a typical characteristic of enantiornithine birds (Chiappe & Walker, 2002). The spatium intermetacarpale is long and narrow and the alular metacarpal is robust and near rectangular in shape. The phalangeal formula of CNU VB-1001 is 2-3-1 and the proximal phalanx of the alular digit becomes gradually slender from its proximal end to its distal end, terminating in a claw which is larger than that of the major digit. The proximal phalanx of the major digit is the broadest among all manual phalanges, and longer than the intermediate phalanx, as in most enantiornithines.

Both femora are poorly preserved, presumably in lateral view, and show no detailed information. The left tibiotarsus, exposed in antero-lateral view, is slightly longer than the femur and has an unfused astragalus with an ascending process on its distal end (Fig. 1). The fibula is expanded proximally, tapers distally, and is nearly half the length of the tibiotarsus. The tarsometatarsus is broad and short, and is nearly half the length of the tibiotarsus. Metatarsal IV is the most slender of the three matatarsals. The pedal digits are well preserved and represent a typical perching anisodactyl foot. Compared with all known enantiornithine birds, the hallux of the new bird is relatively long, approximately 80% of the length of the second digit (Fig. 1); the proximal phalanx is the longest among all non-ungual pedal phalanges. The proximal phalanx of digit 2 is remarkably shorter than the penultimate phalanx. Digit 3 is the longest of the four toes and is nearly the same length as the tarsometatarsus.

DISCUSSION

A series of morphological characters fully show that the new specimen belongs to Enantiornithes, but no character shows it to be a new bird. In general, it is more similar to *Pengornis* than to others, in having a hook-shaped acromion process on the scapula, a large interclavicular angle, a significantly long forelimb (ratio of humerus + ulna + carpometacarpus/femur + tibiotarsus + tarsometatarsus is 1.31, 1.32 in *Pengornis* and the new specimen, respectively), and a large body size (Table 1). The new specimen is different from *Pengornis* by the presence of trabecula

intermedia, a relatively long hallux that is approximately 80% of the length of the second digit, and a more robust ulna.

Avian body size is a characteristic that influences almost all functional processes (Peters, 1983) and, in general, flight performance is often correlated with size reduction – smaller birds are generally more maneuverable in the air and their flight is energetically less expensive. The majority of the known Lower Cretaceous enantiornithines are much smaller than more basal birds (e.g. *Archaeopteryx* and *Confuciusornis*) and this has been taken to represent a remarkable size decrease during the early evolution of birds (Bochenski, 1996; Zhou, 2004). The Jehol enantiornithines *A. wui*, *P. houi*, *X. shenmi*, and *Z. hani* are amongst the four largest known Lower Cretaceous members of this clade (Gong, Hou & Wang, 2004; Zhou *et al.*, 2008; Hu *et al.*, 2012; Zhang *et al.*, 2013). The new bird reported here, although not fully grown at the time of death (evidenced by the absence of fusion between the proximal tarsals and tibia, and the presence of a semilunate carpal that caps the proximal ends of three metacarpals but does not fuse them together), clearly falls within the large-sized region of the spectrum (Table 1), and highlights again that these birds evolved relatively large body sizes early in their evolutionary history (Zhang *et al.*, 2013).

The avian respiratory system is highly derived in lung morphology and ventilatory mechanism. Unlike mammals and other tetrapods, the lungs of birds are rigid and volume-constant during breathing, ventilated mainly by the skeletal movement of the aspiration pump, the rib–sternum complex. Changes in trunk volume, resulting from movements of the sternum and ribs, create pressure differences for lung ventilation. Anatomical features, such as the location of parapophysis and diapophysis on the thoracic vertebrals, uncinate processes and corresponding muscles, bicapitate vertebral ribs, length difference among sternal ribs, and bicondylar sternocostal joint, contribute to greater volumetric changes in the caudal half of the trunk, a key characteristic essential for establishing flow-through ventilation in birds (Codd *et al.*, 2005; Claessens, 2009; Quick & Ruben, 2009). In living birds, the parapophyses lie ventral and cranial to the diapophyses (Fig. 3), and the angle between the two structures generally ranges from 45° to 65°; moreover, the caudal sternal ribs are significantly longer (more than twice as long) than the cranial sternal ribs (Fig. 3); these adaptations of vertebral and rib morphology ensure that the caudal sternal margin is displaced further ventrally than the cranial sternal margin during inspiration, therefore resulting in highly efficient flow-through ventilation. For extinct species, as there are no fossilized soft tissues or lungs, these above-mentioned skeletal adaptations are used

Table 1. Major measurements (mm) of the new material compared with other enantiornithine birds

Species	Hu	Ul	Cmc	Fe	Ti	Tmt	Forelimb/ hindlimb
New material (CNU VB1001)	55.6	60.8	26.4	40.4	44.7	23.0	1.32
Dapingfangornis sentisorhinus (LPM00039)	22	27	11	23	29	16	0.88
Aberratiodontus wui (LHV0001)	–	–	–	55	66.7	33	–
Vescornis hebeiensis (IVPP130722)	23.6	24.8	12.7	23.5	29.8	16.1	0.88
Protopteryx fengningensis (IVPP11665)	27.1	27.3	14.8	19.7	29.6	16.9	1.05
Paraprotopteryx gracilis (STM V001)	22.6	23.5	11.5	22.2	26.3	15.7	0.90
Dalingheornis liweii (CNU VB2005001)	14	14	6	11	16	9	0.94
Eoenantiornis buhleri (IVPP V11537)	35	36	17	32	38	23	0.95
Sinornis santensis (BVP538)	24	–	10.8	–	26.4	14.6	–
Cathayornis yandica (IVPP V9769)	33	34	18	28	34	21	1.02
Shanweiniao cooperorum (D1878/1/2)	22.43	23.36	–	17.6	22.5	11.82	–
Longirostravis hani (IVPP11309)	24	25.5	–	20	25.5	14	–
Longipteryx chaoyangensis (IVPP V12325)	45	47	19	31	32	21	1.32
Pengornis houi (IVPP V15336)	64	71	27	48	50	26	1.31
Cathayornis chabuensis (BMNH-Ph000110)	31.5	32.14	14.02	30.75	35.95	17.18	0.93
Rapaxavis pani (D2522)	22.70	22.88	11.84	19.33	23.24	13.04	1.03
Shenqiornis mengi (D2950)	46.6	46.8	25.5	38.8*	–	25.0	–
Zhouornis hani (CNU VB0903)	50.59	53.79	24.03	44.03	51.62	25.98	1.06
Bohaiornis guoi (LPM B00167)	47	48	22.7	39.0	46.0	22.5	1.09
Parabohaiornis martini (IVPP V 18691)	43.4	43.8	17.6	36	40	19.5	1.10
Longusunguis kurochkini (IVPP V 17964)	40.3	43.6	18.0	35.8	41.8	21.4	1.03
Huoshanornis huji (D2126)	21.3	24.5	13.9	20.8	27.5	15.5	0.94
Sulcavis geeorum (BMNH Ph-000805)	46.5	51.1	–	41.3	47.3	24.3	–
Taxon indet. (CAGS-IG-02-0901)	47.7	49.4	21.5	–	–	–	–

Measurements of *Bohaiornis*, *Parabohaiornis*, *Longusunguis*, and *Sulcavis* are from Wang *et al*., 2014; the others are from Zhang *et al*., 2013. BMNHC, BVP, Beijing Natural History Museum; CAGS, Chinese Academy of Geological Sciences; Cmc, carpometacarpus; CNU, Capital Normal University; D, Dalian Natural History Museum; Fe, femur; Hu, humerus; IVPP, Institute of Vertebrate Paleontology and Paleoanthropology; LHV, Department of Land and Resources of Liaoning Province; LPM, Liaoning Paleontological Museum; STM, Tianyu Natural Museum of Shandong Province; Ti, tibiotarsus; Tmt, tarsometatarsus; Ul, ulna.

as evidence for both a rigid lung and unidirectional airflow in dinosauriformes and pterosaurs (O'Connor & Claessens, 2005; O'Connor, 2006; Codd *et al*., 2008; Claessens, O'Connor & Unwin, 2009; Schachner, Lyson & Dodson, 2009; Schachner *et al*., 2011). Enantiornithines were the dominant bird group in the Mesozoic and had achieved an enhanced flying capacity and control of maneuverability based on the morphology of flight-correlated structures. It is without doubt that the evolution of flight in birds required the development of efficient respiratory and gas-exchange systems (Maina, 2006). However, until now, little information has been available on the lung and lung ventilation in this extinct avian clade.

Uncinate processes were found in the new bird and were also known to exist in *Eoenantiornis*, *Longirostravis*, *Longipteryx*, and *Parabohaiornis* (Zhang *et al*., 2001; Zhou *et al*., 2005; Wang *et al*., 2014). This structure forms an important part of the breathing mechanics of birds because it provides attachment for

appendicocostal muscle, which facilitates movement of the ribs and sternum (Codd *et al*., 2005). The vertebral rib of the new bird presents as a bicapitate structure. In other enantiornithines (e.g. *Neuquenornis*, *Cathayornis*, *Concornis*, *Halimornis*, *Eocathayornis*, *Zhouornis*, *Shenqiornis*, and *Parabohaiornis*), the parapophyses are situated in a mid-central position (Fig. 4), ventral to the diapophyses and dorsal to the lateral excavation of the thoracics. This provides indirect evidence for bicapitate and strongly forked vertebral ribs, and thus rigid and volume-constant lungs in enantiornithine birds. Unlike living birds, whose parapophyses lie cranial and ventral to the diapophyses, these two structures, in enantiornithines, are oriented on the vertical plane, which might suggest that the vertebral rib and corresponding thoracic were set nearly perpendicular to one another and therefore constrained the forward movement of the vertebral rib during inspiration. Length difference among sternal ribs is crucial to sternum movement (Claessens, 2009).
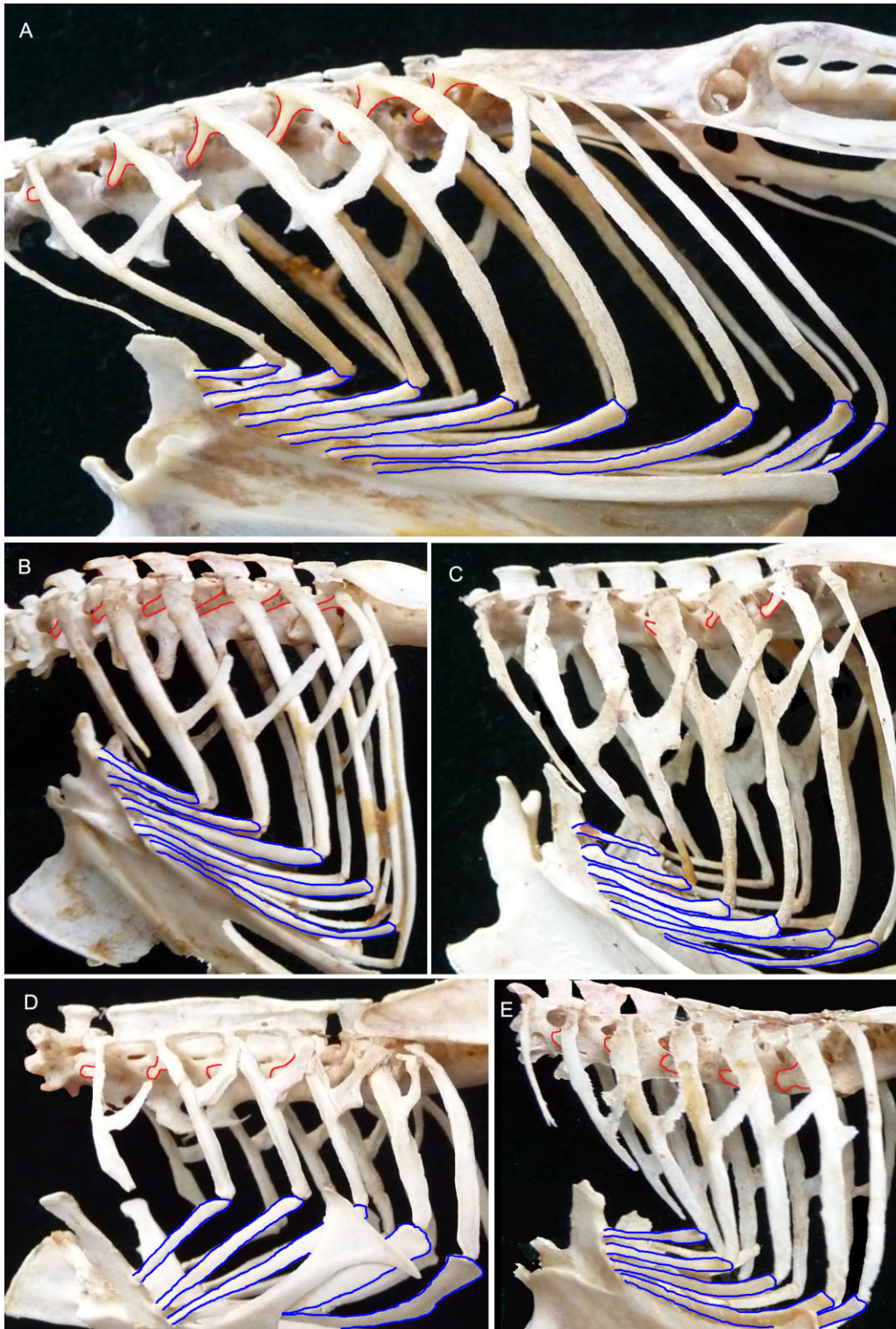
Figure 3. Parapophysis (red/pale grey line) and sternal ribs (blue/dark grey line) of *Anas falcate* (A), *Athene noctua* (B), *Pica pica* (C), *Syrmaticus ellioti* (D), and *Cuculus micropterus* (E). Colour version of figure available online.
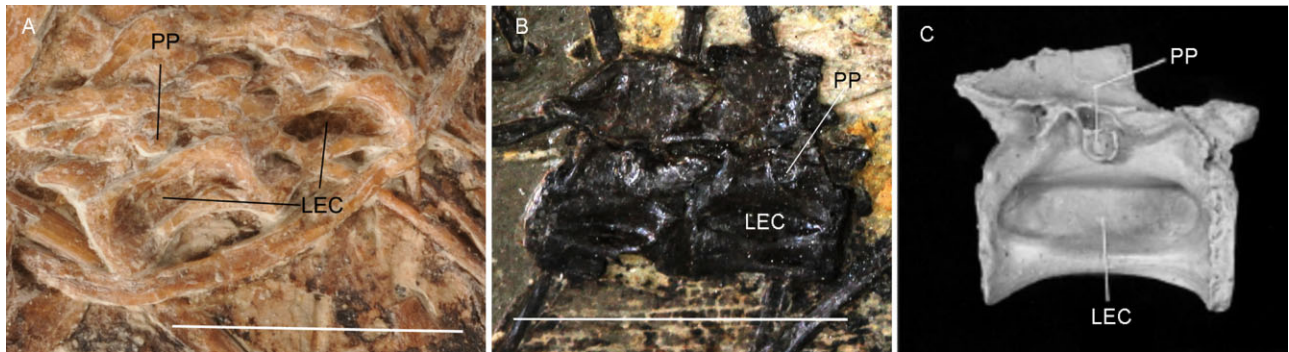
Figure 4. Thoracic vertebrae of *Zhouornis* (A), *Shenqiornis* (B), and *Halimornis* (C). LEC, lateral excavation; PP, parapophysis. Scale bars equal 1 cm.

In extant birds, the ventral displacement of the caudal margin of the sternum is larger than that of the cranial sternal margin, mainly because caudal sternal ribs are significantly longer than cranial sternal ribs (Fig. 3). Unfortunately, the sternal ribs of the new bird are nearly the same in length, as in *Rapaxavis*, *Dalingheornis*, and some juvenile enantiornithines from the Lower Cretaceous in China (Zhang *et al*., 2006; Chiappe, Ji & Ji, 2007; Morschhauser *et al*., 2009). This argues for a relatively smaller volumetric change between the cranial and caudal ends of the rib cage. Taken together, the morphology of the respiratory apparatus, especially the vertebrae and the ribs, might imply that enantiornithines lacked the capacity for higher rates of oxygen consumption and were less efficient than living birds in lung ventilation. This is consistent with histological work, in which enantiornithines were suggested not to be endotherms (Chinsamy, Chiappe & Dodson, 1995; Chinsamy, 2002).

ACKNOWLEDGEMENTS

REFERENCES

Baumel JJ, Witmer LM. 1993. Osteologia. In: Baumel JJ, King AS, Breazile JE, Evans HE, Vanden Berge JC, eds. *Handbook of avian anatomy: nomina anatomica avium, Vol. 23*. Cambridge, MA: Nuttall Ornithological Club, 45–132.

Bochenski Z. 1996. Enantiornithines – a dominant group of the Cretaceous terrestrial birds. *Przeglad Zoologiczny* **40:** 175–184.

Cambra-Moo O, Buscalioni AD, Cubo J, Castanet J, Loth MM, De Margerie E, de Ricqles A. 2006. Histological observations of Enantiornithine bone (Saurischia, Aves) from the Lower Cretaceous of Las Hoyas (Spain). *Comptes Rendus Palevol* **5:** 685–691.

Chiappe LM. 2007. *Glorified dinosaurs: the origin and early evolution of birds*. Hoboken: John Wiley & Sons, Inc., 1–263.

Chiappe LM, Dyke GJ. 2007. The beginnings of birds: recent discoveries, ongoing arguments, and new directions. In: Sues HD, Anderson JS, eds. *Major Transitions in vertebrate evolution*. Bloomington: Indiana University Press, 303–336.

Chiappe LM, Ji S, Ji Q. 2007. Juvenile birds from the Early Cretaceous of China: implications for enantiornithines ontogeny. *American Museum Novitates* **3594:** 1–46.

Chiappe LM, Walker CA. 2002. Skeletal morphology and systematics of the Cretaceous Euenantiornithines (Ornithothoraces: Enantiornithines. In: Chiappe LM, Witmer L, eds. *Mesozoic birds: above the heads of dinosaurs*. Berkeley: University of California Press, 240–267.

Chinsamy A. 2002. Bone microstructure of early birds. In: Chiappe LM, Witmer L, eds. *Mesozoic birds: above the heads of dinosaurs*. Berkeley: University of California Press, 421–431.

Chinsamy A, Chiappe LM, Dodson P. 1995. Mesozoic avian bone microstructure: physiological implications. *Paleobiology* **21:** 561–574.

Claessens LPAM. 2009. The skeletal kinematics of lung ventilation in three basal bird taxa (emu, tinamou, and guinea fowl). *Journal of Experimental Zoology* **311A:** 586–599.

Claessens LPAM, O'Connor PM, Unwin DM. 2009. Respiratory evolution facilitated the origin of pterosaur flight and aerial gigantism. *PLoS One* **4:** 1–8.

Codd JR, Boggs DF, Perry SF, Carrier DR. 2005. Activity of three muscles associated with the uncinate processes of the giant Canada goose *Branta canadensis maximus*. *Journal of Experimental Biology* **208:** 849–857.

Codd JR, Manning PL, Norell MA, Perry SF. 2008. Avian-like breathing mechanics in maniraptoran dinosaurs. *Proceedings of the Royal Society of London B: Biological Sciences* **275:** 157–161.

Dyke GD, Nudds RL. 2009. The fossil record and limb disparity of enantiornithines, the dominant flying birds of the Cretaceous. *Lethaia* **42:** 248–254.

Fedde MR. 1980. The structure and gas flow pattern in the avian lung. *Poultry Science* **59:** 2642–2653.

Gong E, Hou L, Wang L. 2004. Enantiornithine bird with diapsidian skull and its dental development in the Early Cretaceous in Liaoning, China. *Acta Geologica Sinica (English edition)* **78:** 1–7.

He HY, Wang XL, Zhou ZH, Wang F, Boven A, Shi GH, Zhu RX. 2004. Timing of the Jiufotang Formation (Jehol Group) in Liaoning, northeastern China and its implications. *Geophysical Research Letters* **31:** L12605.

Hu D, Xu X, Hou L, Sullivan C. 2012. A new enantiornithine bird from the Lower Cretaceous of Western Liaoning, China, and its implications for early avian evolution. *Journal of Vertebrate Paleontology* **32:** 639–645.

Maina JN. 2006. Development, structure, and function of a novel respiratory organ, the lung–air sac system of birds: to go where no other vertebrate has gone. *Biological Reviews* **81:** 545–579.

Morschhauser EM, Varricchio DJ, Gao C, Liu J, Wang Z, Cheng X, Meng Q. 2009. Anatomy of the Early Cretaceous bird *Rapaxavis pani*, a new species from Liaoning Province, China. *Journal of Vertebrate Paleontology* **29:** 545–554.

O'Connor JK. 2009. A systematic review of Enantiornithes (Aves: Ornithothoraces). PhD dissertation, University of Southern California, Los Angeles, California, 447 pp.

O'Connor PM. 2006. Postcranial pneumaticity: an evaluation of soft-tissue influences on the postcranial skeleton and the reconstruction of pulmonary anatomy in archosaurs. *Journal of Morphology* **267:** 1199–1226.

O'Connor PM, Claessens LPAM. 2005. Basic avian pulmonary design and flowthrough ventilation in nonavian theropod dinosaurs. *Nature* **436:** 253–256.

Peters RH. 1983. *The ecological implication of body size*. Cambridge: Cambridge University Press.

Powell FL. 2000. Respiration. In: Causey Whittow G, ed. *Sturkie's avian physiology, 5th edition*. San Diego: Academic Press, 233–264.

Quick DE, Ruben JA. 2009. Cardio-pulmonary anatomy in theropod dinosaurs: implications from extant archosaurs. *Journal of Morphology* **270:** 1232–1246.

Ruben JA, Jones TD, Geist NR. 2003. Respiratory and reproductive paleophysiology of dinosaurs and early birds. *Physiological and Biochemical Zoology* **76:** 141–164.

Ruben JA, Jones TD, Geist NR, Hillenius WJ. 1997. Lung structure and ventilation in theropod dinosaurs and early birds. *Science* **278:** 1267–1270.

Schachner ER, Farmer CG, McDonald ZT, Dodson P. 2011. Evolution of the dinosauriform respiratory apparatus: new evidence from the postcranial axial skeleton. *The Anatomical Record* **294:** 1532–1547.

Schachner ER, Lyson TR, Dodson P. 2009. Evolution of the respiratory system in nonavian theropods: evidence from rib and vertebral morphology. *The Anatomical Record* **292:** 1501–1513.

Tickle PG, Norell MA, Codd JR. 2012. Ventilatory mechanics from maniraptoran theropods to extant birds. *Journal of Evolutionary Biology* **25:** 740–747.

Wang M, Zhou ZH, O'Connor JK, Zelenkov NV. 2014. A new diverse enantiornithine family (Bohaiornithidae fam. nov.) from the Lower Cretaceous of China with information from two new species. *Vertebrata PalAsiatica* **52:** 31–76.

Wang X, Zhang ZH. 2011. Enantiornithine birds in China. *Acta Geologica Sinica (English edition)* **85:** 1211–1223.

Zhang FC, Zhou ZH. 2000. A primitive enantiornithine bird and the origin of feathers. *Science* **290:** 1955–1959.

Zhang FC, Zhou ZH, Hou LH, Gu G. 2001. Early diversification of birds: evidence from a new opposite bird. *Chinese Science Bulletin* **46:** 945–949.

Zhang ZH, Chiappe LM, Han G, Chinsamy A. 2013. A large bird from the Early Cretaceous of China: new information on the skull of enantiornithines. *Journal of Vertebrate Paleontology* **33:** 1176–1189.

Zhang ZH, Hou LH, Hasegava Y, O'Connor J, Martin LD, Chiappe LM. 2006. The first Mesozoic heterodactyl bird from China. *Acta Geologica Sinica (English edition)* **80:** 631–635.

Zheng X, O'Connor J, Huchzermeyer F, Wang X, Wang Y, Wang M, Zhou Z. 2013. Preservation of ovarian follicles reveals early evolution of avian reproductive behaviour. *Nature* **495:** 507–511.

Zhou ZH. 2004. The origin and early evolution of birds: discoveries, disputes, and perspectives from fossil evidence. *Die Naturwissenschaften* **91:** 455–471.

Zhou ZH, Chiappe LM, Zhang FC. 2005. Anatomy of the Early Cretaceous bird *Eoenantiornis buhleri* (Aves: Enantiornithines) from China. *Canadian Journal of Earth Sciences* **42:** 1331–1338.

Zhou ZH, Clarke J, Zhang FC. 2008. Insight into diversity, body size and morphological evolution from the largest Early Cretaceous enantiornithine bird. *Journal of Anatomy* **212:** 565–577.